DALTON
FULL PAPER

Reactivity of the $[MoS_4Cu_6Br_8]^{4-}$ anion toward polyarylphosphorus ligands: synthesis, characterization and nonlinear optical properties of $[MoS_4(Cudppf)_2]\cdot 2DMF\cdot CH_3CN$ and $[MoS_4Cu_2(Ph_2PPy)_4]$

Yun-Yin Niu,[a] Tian-Niu Chen,[b] Shi-Xiong Liu,[c] Ying-Lin Song,[d] Yu-Xiao Wang,[d] Zi-Ling Xue[b] and Xin-Quan Xin*[a]

[a] *State Key Laboratory of Coordination Chemistry, Coordination Chemistry Institute, Nanjing University, Nanjing 210093, P. R. China*
[b] *Department of Chemistry, University of Tennessee, Knoxville, TN 37996-1600, US*
[c] *Central Laboratory of Fuzhou University, Fuzhou 350002, P. R. China*
[d] *Harbin Institute of Technology, Harbin 150001, P. R. China*

Received 9th October 2001, Accepted 20th February 2002
First published as an Advance Article on the web 8th April 2002

$[NH_4]_2[MoS_4]$ reacts with CuBr and $[Bu_4N]Br$ in the solid state to afford an intermediate product with proposed constitution $[Bu_4N]_4[MoS_4Cu_6Br_8]$ (**1**). Treatment of cluster (**1**) with an equal equivalent of dppf in CH_3CN–DMF solution resulted in the formation of a pentanuclear cluster $[MoS_4(Cudppf)_2]\cdot 2DMF\cdot CH_3CN$ (**2**). Cluster (**2**) crystallizes in the monoclinic space group $P2_1/n$ with four formula units in a cell of dimensions $a = 13.1267(8)$, $b = 38.040(2)$, $c = 15.2661(9)$ Å, and $\beta = 97.6030(10)°$. Refinement by full-matrix least-squares techniques gave final residuals $R = 0.0567$ and $wR = 0.1679$. The structure of (**2**) can be described as two $(Cudppf)^+$ units linked through MoS_4^{2-} to form a pentanuclear folding-ruler array. Reaction of (**1**) with excess Ph_2PPy in CH_3CN solution resulted in the formation of a trinuclear cluster $[MoS_4Cu_2(Ph_2PPy)_4]$ (**3**). Cluster (**3**) crystallizes in the tetragonal space group $I4_1/a$ with cell constants $a = 17.427(6)$, $b = 17.427(6)$, $c = 21.344(5)$ Å, and $Z = 4$. Final residuals $R = 0.0337$ and $wR = 0.0616$. The structure of (**3**) is built up from two $Cu(Ph_2PPy)_2^+$ units bridged by a MoS_4^{2-} ligand to form a trinuclear symmetrical linear molecule. Clusters (**2**) and (**3**) exhibit strong optical absorption (effective $\alpha_2 = 1.6 \times 10^{-9}$ m W^{-1} (**2**) and 1.2×10^{-9} m W^{-1} (**3**)) and optical self-defocusing effects ($n_2 = -1.35 \times 10^{-17}$ m^2 W^{-1} (**2**) and -6.84×10^{-17} m^2 W^{-1} (**3**)), their limiting thresholds were determined to be 0.35 J cm^{-2} (**2**) and 0.65 J cm^{-2} (**3**), which are about four and two times, respectively, better than that of C_{60}.

Introduction

The chemistry of transition metal–sulfur clusters[1,2] has attracted much interest recently owing to their relevance to certain biological and industrial catalysts,[3,4] rich structural chemistry,[5] and special reactive properties[6] as well as potential application in nonlinear optical materials.[7–9] We recently reported a heptanuclear cluster $[Bu_4N]_4[MoS_4Cu_6Br_8]$ (**1**).[10] The structure of the anion was concluded and described as an octahedral core in which the Br^- groups are labile and many monodentate σ-donor ligands such as PPh_3 can be conveniently introduced into cluster species by ligand substitution. The goal of the reactions, however, is not simply to generate novel compounds, rather, it is to study and understand the relationship between the cluster structure, especially the peripheral ligands and nonlinear optical properties. Due to the similarity in aromaticity for benzene, pyridine and ferrocene, dppf and Ph_2PPy were selected to use for this purpose.

Although the coordination chemistry of dppf[11] and Ph_2PPy[12] is well developed, the corresponding chemistry with heterothiometallate clusters has received less attention. No fewer than ten trinuclear heterothiometallate species of the composition $[(PR_3)_nM'_2MS_4]$ ($PR_3 = PPh_3$, $MePPh_2$; M = Mo, W; M′ = Cu, Ag, Au; $n = 2$, 3, 4) have been studied due to their rich symmetrical nature.[13–14] Most of the compounds belong to the case of $n = 2$–3 while the symmetrical species of $n = 4$ have never been purely isolated and structurally characterized by X-ray determination.[15,16] In the present work we have used the lability of the Br^- ligands in $[Bu_4N]_4[MoS_4Cu_6Br_8]$ (**1**) to afford a new complex of the dppf ligand $[MoS_4(Cudppf)_2]\cdot 2DMF\cdot CH_3CN$ (**2**) and a complex of Ph_2PPy, $[MoS_4Cu_2(Ph_2PPy)_4]$ (**3**). Charge transfer excited states are the origin of optical nonlinearity. This incorporation of metal atoms in the electronic structure may result in the involvement of metal d orbitals in the optical charge-transfer process and effects on the nonlinear optical properties.[17] Because phosphine ligands containing ferrocenyl or pyridyl moieties possess electron-donor characteristics[18–19] and heterothiometallate clusters exhibit "electron-poor" characteristics,[14,20] we reasoned that the combination of above characteristics might lead to a molecule with a considerable inner optical charge transfer or NLO properties.

Experimental

Materials and syntheses

All syntheses were performed in oven-dried glassware under a purified nitrogen atmosphere using standard Schlenk techniques. The solvents were purified by conventional methods and degassed prior to use. All elemental analyses were carried out by the Analytical Center of Nanjing University. $[Bu_4N]_4[MoS_4Cu_6Br_8]$ (**1**) was prepared by an improvement on the literature method.[10] Dppf and Ph_2PPy were purchased from Aldrich. Solvents and other reagents were obtained commercially and were used without further purification.

Instrumentation

Electronic absorption spectra were obtained on a Shimazu UV-3000 spectrophotometer. Infrared spectra were recorded

 DOI: 10.1039/b109103d

on an FTS-40 spectrophotometer with the use of pressed KBr pellets. ^{1}H NMR and ^{31}P NMR spectra were recorded on a Bruker ACF300 FT-NMR instrument using TMS as internal reference at 25 °C in CD_2Cl_2. Carbon, hydrogen and nitrogen analyses were performed on a PE-240 elementary analyser. Molybdenum and copper analyses were performed on a JA-1100 ICP spectrophotometer.

Preparation of $[MoS_4(Cudppf)_2]\cdot 2DMF\cdot MeCN$ (2)

A solution of (**1**) (1.107 g, 0.5 mmol) in MeCN (5 mL) was added dropwise to a solution of dppf (0.275 g, 0.5 mmol) in DMF (15 mL). The mixture was stirred at 60 °C for 30 minutes and then filtered to afford a purple–red filtrate. Air-stable black–red microcrystals of (**2**) were obtained by slow evaporation of the solution in five days. They were washed with MeCN and Et_2O, dried under vacuum to give 0.33 g of (**2**), yield 40%. (Found: C, 55.36; H, 4.40; N, 2.55; Cu, 7.55; Mo, 5.90. Calc. for $C_{76}H_{73}Cu_2Fe_2MoN_3O_2P_4S_4$: C, 55.37; H, 4.47; N, 2.55; Cu, 7.64; Mo, 5.94). ^{1}H NMR (CD_2Cl_2): δ, ppm 4.08(s, 4H, C_5H_4), 4.37(s, 4H, C_5H_4), 4.54(s, 4H, C_5H_4), 4.57(s, 4H, C_5H_4), 7.10–7.75(m, 40H, $4C_6H_5$). ^{31}P NMR (CD_2Cl_2), δ, ppm 5.54(m). UV-vis (DMF, λ_{max}/nm, 10^{-3} ε/M^{-1} cm^{-1}): 492 (6.72), 370(8.50), 317 (8.91). IR (cm^{-1}): 1675.6(s, $\nu_{C=O}$), 1479.9(m), 1434.2(s), 1384.8(m), 1164.5(m), 1094.4(s), 1069.7(m), 1028.5(s), 820.77(m), 743.09(s), 696.02(s), 511.97(m), 486.56(m), 469.25(s), 440.08(m, $\nu_{Mo-\mu-S}$), 424.46(m).

Preparation of $[MoS_4Cu_2(Ph_2PPy)_4]$ (3)

A solution of (**1**) (1.107 g, 0.5 mmol) in MeCN (5 mL) was added dropwise to a solution of 2-(diphenylphosphino)pyridine (0.792 g, 3.0 mmol) in MeCN (15 mL). A large amount of black–red microcrystals of (**2**) were obtained by slow evaporation of the clear solution in five days, the crystals were washed with EtOH and Et_2O, dried under vacuum to give 0.41 g of (**3**), yield 59%. (Found: C, 58.02; H, 4.02; N, 4.01; Cu, 8.80; Mo, 6.50. Calc. for $C_{68}H_{56}Cu_2MoN_4P_4S_4$: C, 58.16; H, 4.02; N, 3.99; Cu, 8.96; Mo, 6.97). ^{1}H NMR (CD_2Cl_2):δ, ppm 6.45(m, 8H, $H_{4,4',4'',4'''}$ + $H_{5,5',5'',5'''}$), 6.88(d, 4H, $H_{3,3',3'',3'''}$), 8.35(d, 4H, $H_{6,6',6'',6'''}$). 7.04–7.9(m, 40H, $8C_6H_5$). ^{31}P NMR (CD_2Cl_2), δ, ppm 14.1(m).UV-vis (DMF, λ_{max}/nm, 10^{-3} ε/M^{-1} cm^{-1}): 490.5(3.98), 371 (6.22). IR (cm^{-1}): 3047.1(s), 1572.1(s), 1560.7(m), 1480.4(m), 1454.3(m), 1433.8(s), 1420.2(m), 1093.4(m), 991.7(m), 772.5(m), 740.5(s), 692.9(s), 517.7(s), 508.9(s), 491.4(m), 463.6(s), 442.7(m, $\nu_{Mo-\mu-S}$).

Nonlinear opticals

The optical measurements were performed with linearly polarized 7 ns pulses at 532 nm generated from a frequency-doubled Q-switched Nd:YAG laser, this wavelength is of paramount practical importance in the field of optical limiting as well as design and fabrication of resonance cavities of lasers. The spacial profiles of the pulses were nearly Gaussian after a spatial filter was employed. A DMF solution of compound (**2**) or (**3**) was placed in a 1-mm-thick quartz cell for optical limiting measurements. The crystal samples of each compound are stable toward oxygen, moisture and laser light. The laser beam was focused with a 25 cm focal-length focusing mirror. The radius of the beam circumference was measured to be 30 ± 5 μm (half-width at $1/e^2$ maximum in irradiance). The incident and transmitted pulse energy were measured simultaneously by two energy detectors (Laser Precision Rjp-735) which were linked to a computer by an IEEE interface.[21–22] The interval between the laser pulses was chosen to be ~5 s for operational convenience and controlled by the computer. The NLO properties of sample (**2**) and (**3**) were manifested by moving the sample along the axis of the incident laser beam (*Z*-direction) with respect to the focal point instead of being positioned at its focal point, and an identical setup was adopted in the experiments to measure the *Z*-scan data. An aperture of 0.5 mm radius was placed in front of the detector to assist the measurement of the nonlinear optical refraction effect.

Crystallographic studies

The structure of (**2**) was determined by the single-crystal X-ray diffraction method. Intensity data for the compound was collected on a Bruker AXS Smart 1000 X-ray diffractometer equipped with a CCD area detector, graphite-monochromated Mo radiation (K_α = 0.71073 Å) and an upgraded Nicolet LT-2 low temperature device. A suitable crystal was coated with paratone oil (Exxon) and mounted on a glass fiber under a stream of nitrogen at 173(2) K. Data collection nominally covered over a hemisphere of reciprocal space by combining four sets of exposures. Each of the first three sets had a different φ angle (0, 120 and 240°) with each exposure covering 0.3° in ω. The fourth set was a φ-scan with each exposure covering 0.3° in φ. Unit cell refinement and data reduction were performed by SAINT,[23] and an empirical absorption correction applied (SADABS).[24] The structures were solved by direct methods, and expanded using Fourier techniques (SHELXTL).[25] All non-hydrogen atoms were refined anisotropically except for those in the disordered solvents *N*,*N*-dimethylformamide (DMF) and acetonitrile (MeCN) (C69–C76, N1–N3, O1–O2), which were only refined isotropically. Hydrogen atoms were placed in calculated positions. A summary of parameters associated with the structure determinations is given in Table 1. Selected bond distances and angles are listed in Table 2. An ORTEP diagram of (**2**) is shown in Fig. 1.

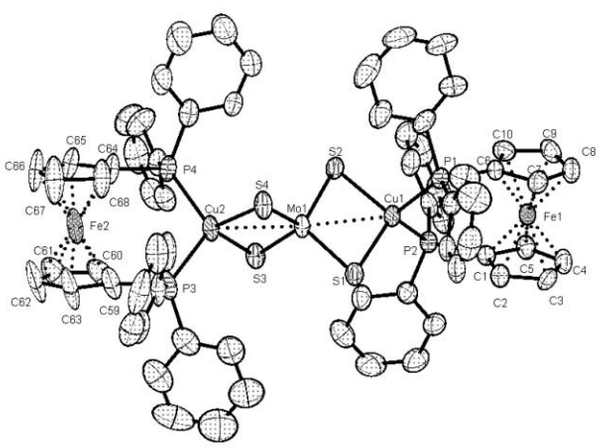

Fig. 1 ORTEP view of $[MoS_4(Cudppf)_2]\cdot 2DMF\cdot CH_3CN$ (**2**), showing 50% thermal ellipsoids. All H atoms and atoms belonging to disordered solvents are omitted, all labels for carbons in the phenyl rings are turned off for clarity.

A black–red prismatic crystal of (**3**) was mounted on a glass fiber. All measurements were on a Rigaku R-AXIS RAPID Weissenberg IP diffractomer with graphite-monochromated Mo Kα radiation (λ = 0.71069 Å), the scan mode being ω. The data reductions were performed on a Silicon Graphics Indy workstation with Smart-CCD software.[26] An ψ empirical absorption correction was applied.[27] The structure was solved by direct methods and refined by full-matrix least squares on F^2 using the SHELXTL-PC (Version 5.1) package.[28] All non-hydrogen atoms were refined anisotropically. All hydrogen atoms were placed in their calculated positions for C–H in C_6H_5 groups or from a difference Fourier map for C–H in pyridine, respectively. Their contributions were included in the structure factor calculations. A summary of parameters associated with the structure determinations is given in Table 1. Selected bond distances and angles are listed in Table 2. An ORTEP diagram of (**3**) is shown in Fig. 3.

Table 1 Crystal data and structure refinement for $[MoS_4(Cudppf)_2]\cdot 2DMF\cdot CH_3CN$ (**2**) and $[MoS_4Cu_2(Ph_2PPy)_4]$ (**3**)

	(**2**)	(**3**)
Empirical formula	$C_{76}H_{73}Cu_2Fe_2MoN_3O_2P_4S_4$	$C_{68}H_{56}Cu_2MoN_4P_4S_4$
M	1647.21	1404.31
T/K	173(2)	293(2)
Wavelength/Å	0.71073	0.71073
Crystal size/mm^3	0.32 × 0.24 × 0.19	0.21 × 0.21 × 0.16
Crystal system	Monoclinic	Tetragonal
Space group	$P2_1/n$	$I4_1/a$
a/Å	13.1267(8)	17.4276(15)
b/Å	38.040(2)	17.4276(15)
c/Å	15.2661(9)	21.3445(19)
β/°	97.6030(10)	90
V/Å^3	7556.0(8)	6482.8(10)
Z	4	4
ρ_{Calc}/g cm^{-3}	1.448	1.439
μ/mm^{-1}	1.331	1.112
F(000)	3368	2864
Goodness-of-fit on F^2	1.167	0.678
$R1$ [a]	0.0567	0.0337
$wR2$ [b]	0.1679	0.0616

[a] $R = \Sigma \left|\, |F_o| - |F_c| \,\right| / \Sigma |F_o|$. [b] $wR = [\Sigma w(|F_o^2| - |F_c^2|)^2 / \Sigma w |F_o^2|^2]^{1/2}$.

Table 2 Selected bond distances (mean distances and range, [Å]) and bond angles [°] for $[MoS_4(Cudppf)_2]\cdot 2DMF\cdot CH_3CN$ (**2**) and $[MoS_4Cu_2(Ph_2PPy)_4]$ (**3**)

	(**2**)	(**3**)
Mo–S	2.199(5)	2.204(8)
Mo–Cu	2.753(7)	2.785(1)
Cu–S	2.300(5)	2.304(4)
Cu–P	2.304(6)	2.302(1)
P–C	1.823(1)	1.828(3)
Cu–Fe	4.079(2)	
Fe–C	2.043(7)	
P–Cu–P	111.52(2)	112.99(4)
Cu–Mo–Cu	173.44(3)	180.0
Mo–Cu ··· Fe	174.65(8)	

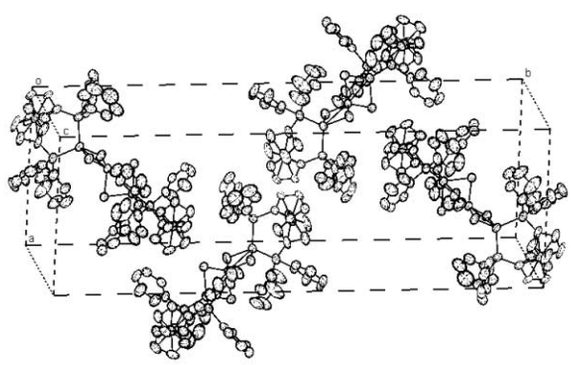

Fig. 2 Packing diagram of $[MoS_4(Cudppf)_2]\cdot 2DMF\cdot CH_3CN$ (**2**) along the c axis. All solvent molecules and hydrogen atoms are omitted for clarity.

CCDC reference numbers 164998 and 174883.

See http://www.rsc.org/suppdata/dt/b1/b109103d/ for crystallographic data in CIF or other electronic format.

Results and discussion

Structural description

Mo–S stretching vibrations for (**2**) and (**3**) were found at about 440.08 and 442.7 cm^{-1}, respectively. These vibrations belong to characteristic Mo–μ-S bonding mode, suggesting that no other S-coordination (t-S or μ_3-S) exists.[14]

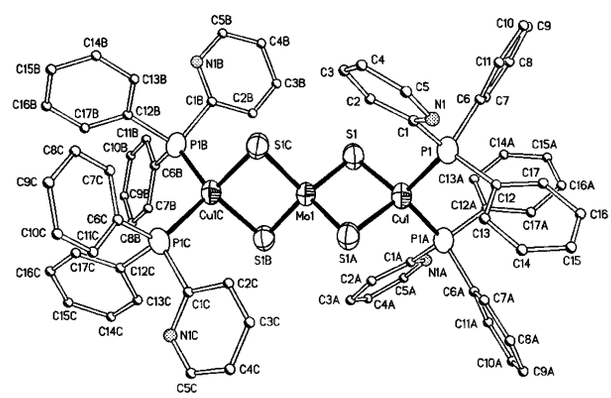

Fig. 3 Drawing of $[MoS_4Cu_2(Ph_2PPy)_4]$ (**3**) with 50% displacement ellipsoids. All H atoms are omitted for clarity.

The structures of (**2**) and (**3**) were confirmed by an X-ray diffraction study. Fig.1 and Fig. 2 show the structure and packing diagram, respectively, of $[MoS_4(Cudppf)_2]\cdot 2DMF\cdot CH_3CN$ (**2**). In (**2**) a MoS_4^{2-} group forms a bridge between two $(Cudppf)^+$ units. The geometry around Mo in (**2**) is a slightly distorted tetrahedron (107.71(7)–111.26(7)°). The deviation from tetrahedral geometry around Mo is close to that in the monodentate ligand-containing cluster $[(PPh_3)_3Cu_2MoS_4\cdot 0.8CH_2Cl_2]$.[29] The geometry around Cu is a distorted tetrahedron with S–Cu–S(P) angles of 100.88(7)–115.20(7)°. However a distinct difference between (**2**) and a common linear cluster originates from the nonlinear arrangement of the five metal atoms, with the Cu ··· Mo ··· Cu and Mo ··· Cu ··· Fe angles deviating 7 and 5° from 180° respectively. The Cu–P bond lengths (mean 2.304(6) Å) are in agreement with the corresponding Cu–P bond lengths in $[(PPh_3)_3Cu_2MoS_4\cdot 0.8CH_2Cl_2]$ (av. 2.30(3) Å for 4-coordinated copper).[29] The average Mo–Cu and Cu–S distances in (**2**) agree well with those in other linear heterothiometallic compounds.[29,30]

The molecular structure of (**3**) is shown in Fig. 3 and selected bond lengths and angles are given in Table 2. The molecule has a crystallographically imposed −4 symmetry of four-fold rotation-inversion. The molybdenum atom located at −4 has essentially tetrahedral coordination geometry. Each copper atom located at 2[001] also has tetrahedral geometry, being bonded to two phosphorus atoms and two sulfur atoms. Main bond distances and angles in this compound are unexceptional and comparable to those in (**2**) with the exception of the

collinear trimetal centers (Cu ··· Mo ··· Cu = 180.0°). Interestingly due to the presence of the uncoordinated nitrogen atoms on the pendant Ph_2PPy ligands, a potential reactive activity may be expected for (**3**).[12]

Although the formation mechanism of these two linear clusters with four-coordinate coppers is not clear, a possible axial nucleophilic attack of tertiary phosphine ligands may cause the collapse of the octahedron core MoS_4Cu_6. There have been studies indicating that steric factors are also the dominant influence in determining the reactivities of the triaromatic phosphine toward transition metals.[31] In these two clusters the Cu–P distances are slightly longer than those in Cu(I)–PPh_3 complexes [mean 2.264(3) Å in $\{(PPh_3)_2CuN_3\}_2$][32] and the P–Cu–P bond angles are smaller than those in Cu(I)–PPh_3 [mean 121.5(6)° in $\{(PPh_3)_2CuN_3\}_2$], which appears to optimize the rigid MoS_4^{2-} anion tetrahedron and minimize the non-bonded repulsions between the phenyl rings.[33]

Nonlinear optical properties

The nonlinear optical properties of $[MoS_4(Cudppf)_2]\cdot 2DMF\cdot CH_3CN$ (**2**) and $[MoS_4(Cu_2(Ph_2PPy)_4]$ (**3**) were investigated using the *Z*-scan technique.

Fig. 4a and Fig. 5a show typical *Z*-scan measurements of

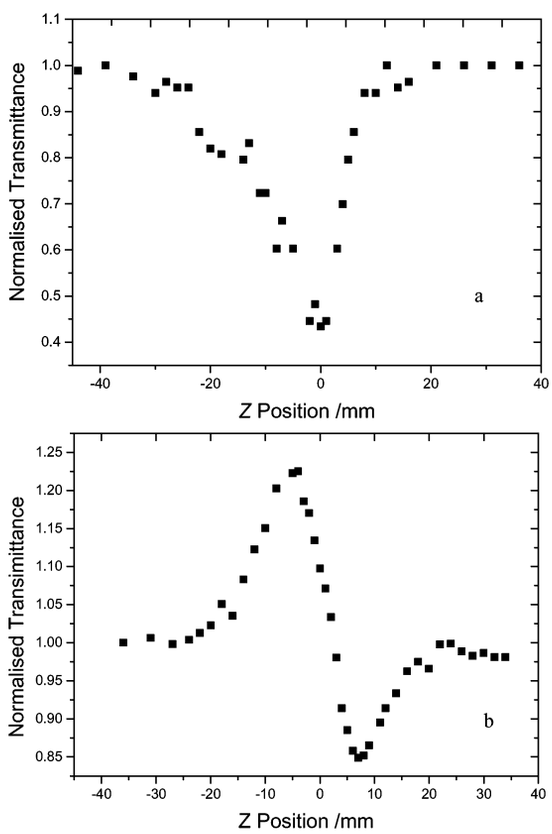

Fig. 4 *Z*-scan data (filled boxes) of $[MoS_4(Cudppf)_2]\cdot 2DMF\cdot CH_3CN$ (**2**) in a 1.3×10^{-4} mol dm^{-3} DMF solution at 532 nm with $I(Z = 0)$ being 1.2×10^{12} W m^{-2} (a) collected under open aperture configuration showing NLO absorption. (b) obtained by dividing the normalized *Z*-scan data obtained under closed aperture configuration by the normalized *Z*-scan data (a). It shows the self-defocusing effect of the cluster.

(**2**) in a 1.3×10^{-4} mol dm^{-3} DMF solution and (**3**) in a 1.55×10^{-4} mol dm^{-3} DMF solution, respectively. The filled boxes are the experimental data measured under an open aperture. The data clearly illustrate that the absorption increases as the incident light irradiance rises. The solid lines are the theoretical curves from the classical equations.[34] The effective nonlinear absorptive index α_2 is estimated to be 1.6×10^{-9} mW^{-1} (**2**) and 1.2×10^{-9} mW^{-1} (**3**).

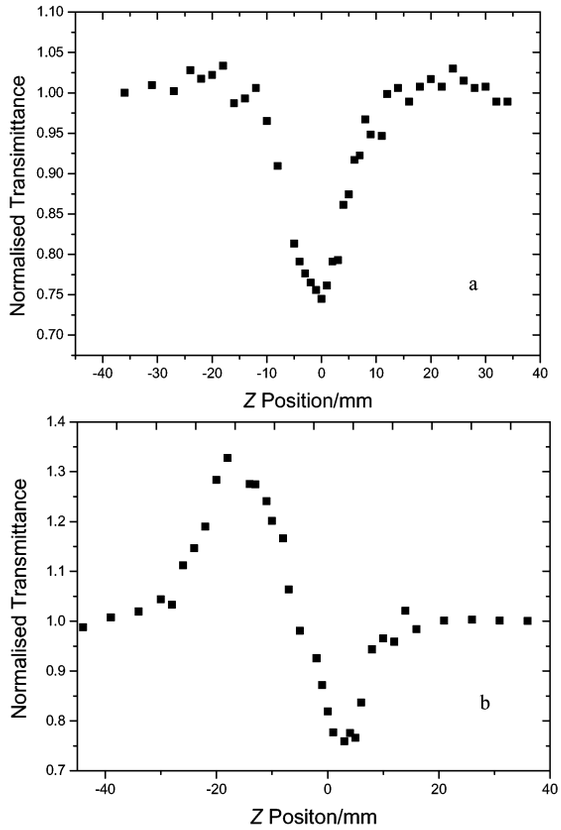

Fig. 5 *Z*-scan data (filled boxes) of $[MoS_4Cu_2(Ph_2PPy)_4]$ (**3**) in a 1.55×10^{-4} mol dm^{-3} DMF solution at 532 nm with $I(Z = 0)$ being 1.2×10^{12} W m^{-2} (a) collected under open aperture configuration showing NLO absorption. (b) obtained by dividing the normalized *Z*-scan data obtained under closed aperture configuration by the normalized *Z*-scan data of (a). It shows the self-defocusing effect of the cluster.

The nonlinear refractive components of the compound were assessed by dividing the normalized *Z*-scan data obtained under closed aperture configuration by the normalized *Z*-scan data collected under open aperture configuration (Fig. 4b and Fig. 5b). The data show that these two clusters have a negative sign for refractive nonlinearity, the valley/peak pattern of the normalized transmittance curve shows characteristic self-defocusing behavior of the propagating light in the sample. The n_2 value was estimated from these data to be -1.35×10^{-17} for (**2**) and -6.84×10^{-17} m^{2}W^{-1} for (**3**), respectively. The nonlinear refractive self-defocusing behavior is comparable to linear cluster $[MoAu_2S_4(AsPh_3)_2]$ ($n_2 = -5.1 \times 10^{-17}$ m^{2}W^{-1})[35] and twin-nest cluster $[Et_4N]_4[Mo_2O_2S_6Cu_6I_6]$ (-6×10^{-17} m^2 W^{-1}).[36]

The optical limiting effects of clusters (**2**) and (**3**) are depicted in Fig. 6. The peak fluence for *Z*-scan is about 1 J cm^{-2} in ns *Z*-scan. The transmittance is normalized to its linear transmittance at low incident fluence. The results for the two clusters, which have a similar MoS_4Cu_2 cluster skeleton, demonstrate that the optical limiting capacity of (**2**) is obviously better than that of (**3**). At very low fluence they respond linearly to the incident light fluence obeying Beer's law. The light transmittance starts to deviate from Beer's law of the linear response when the input light fluence rises to certain values with respect to each cluster. From the optical limiting experimental data, the values of the limiting threshold are measured as 0.35 J cm^{-2} and 0.65 J cm^{-2} for cluster (**2**) and (**3**), respectively. These values are four and two times, respectively, better than the 1.6 J cm^{-2} limiting threshold of C_{60}.[37] Lower limiting thresholds and saturation levels provide greater safety margin for device protection. The challenging question is why these clusters can perform better than C_{60} and other clusters with cage structure. Previous study has shown that the skeletal structure and constituent metal nuclearity play an important role in determining their NLO

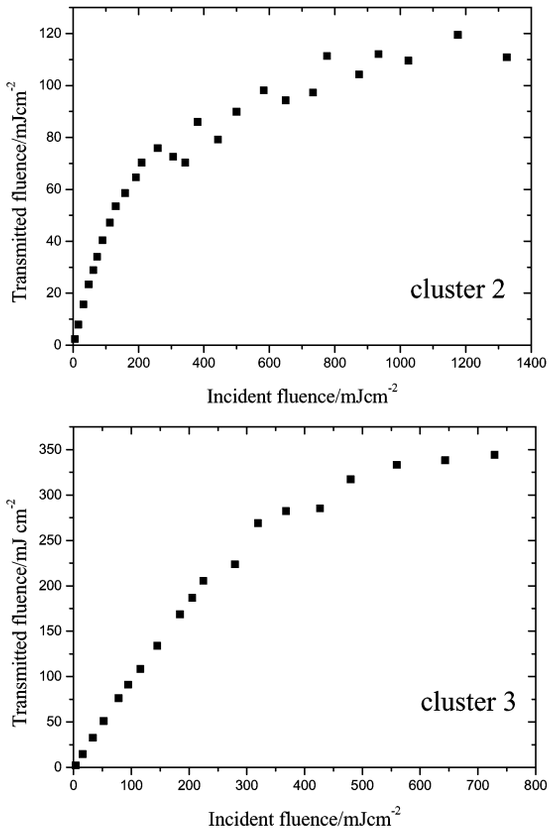

Fig. 6 Optical limiting effect of $[MoS_4(Cudppf)_2]\cdot 2DMF\cdot CH_3CN$ (**2**) (1.3×10^{-4} mol dm^{-3} and $[MoS_4Cu_2(Ph_2PPy)_4]$ (**3**) (1.55×10^{-4} mol dm^{-3}) in DMF solution.

properties. Clusters with higher symmetry or nuclearity are expected to have favorable NLO properties.[7] As far as clusters (**2**) and (**3**) are concerned, although they don't possess these two advantages, unexpectedly they are still better than most clusters; cluster (**2**) is even comparable to (or slightly better than) some of the known good optical limiting materials, which possess a pentanuclear 'open' structure.[38]

In conclusion, we have successfully synthesized and structurally characterized two typical copper heterothiometallic clusters through the rational molecular design method. Different from general synthesizing approaches, both clusters are constructed by reaction of an intermediate precursor with arylphosphorus ligands. Both exhibit optical self-defocusing effects and large optical limiting effects. The results of this study indicate that rational molecular design may bring us brand-new knowledge on the nonlinear optics of metalloorganic compounds. Further studies are in progress, which are directed at studying the metalloorganic ligands, tuning the NLO properties and incorporating these groups into cluster hosts in order to obtain novel structure types, especially the planar "open" motifs.[39] Therefore, we shall try to design and synthesize additional heterothiometallic clusters to explore the structure–property and ligand–property relationship until their structures and optical properties can be predicted and controlled.

Acknowledgements

This project was supported by the National Science Foundation (No. 29631040) of China.

References

1 E. I. Stiefel and K. Matsumoto, *Transition Metal Sulfur Chemistry: Biological and Industrial Significance*, American Chemical Society, Washington, DC, 1996.
2 S. C. Lee and R. H. Holm, *Angew. Chem., Int. Ed. Engl.*, 1990, **29**, 840.
3 J. Kim and D. C. Rees, *Science*, 1992, **257**, 1677.
4 D. Coucouvanis, *Acc. Chem. Res.*, 1991, **24**, 1.
5 (*a*) H. Kawaguchi, K. Yamada, J.-P. Lang and K. Tatsumi, *J. Am. Chem. Soc.*, 1997, **119**, 10346; (*b*) J. Han, K. Beck, N. Ockwig and D. Coucouvanis, *J. Am. Chem. Soc.*, 1999, **121**, 10448.
6 (*a*) Y.-Y. Niu, Y.-L. Song, H.-G. Zheng, F. Li, H.-K. Fun and X.-Q. Xin, *New J. Chem.*, 2001, **25(7)**, 945; (*b*) Q.-F. Zhang, Y.-Y. Niu, W. H. Leung, Y.-L. Song, I. D. Williams and X.-Q. Xin, *Chem. Commun.*, 2001, 1126; (*c*) V. Bereau, C. G. Pernin and J. A. Ibers, *Inorg. Chem.*, 2000, **39**, 854.
7 S. Shi, W. Ji, S.-H. Tang, J.-P. Lang and X.-Q. Xin, *J. Am. Chem. Soc.*, 1994, **116**, 3615.
8 H.-W. Hou, X.-R. Ye, X.-Q. Xin, J. Liu, M.-Q. Chen and S. Shi, *Chem. Mater.*, 1995, **7**, 472.
9 S. Shi, W. Ji and X.-Q. Xin, *J. Phys. Chem.*, 1995, **99**, 894.
10 J. P. Lang, X. Q. Xin and K. B. Yu, *J. Coord. Chem.*, 1994, **33**, 99 and references therein.
11 K. S. Gan and T. S. A. Hor, in *Ferrocenes. Homogeneous Catalysis, Organic Synthesis and Materials Science*, ed. A. Togni and T. Hayashi, VCH, Weinheim, 1995, ch. 1; and references therein.
12 G. Francio, R. Scopelliti, C. G. Arena, G. Bruno, D. Drommi and F. Faraone, *Organometallics*, 1998, **17**, 338.
13 H.-W. Hou, X.-Q. Xin and S. Shi, *Coord. Chem. Rev.*, 1996, **153**, 25.
14 C. Zhang, G.-C. Jin, J.-X. Chen, X.-Q. Xin and K.-P. Qian., *Coord. Chem. Rev.*, 2001, **213**, 51.
15 S. Sarkar and S. B. S. Mishra., *Coord. Chem. Rev.*, 1984, **59**, 239.
16 A. Müller, E. Diemann, R. Jostes and H. Bögge., *Angew. Chem., Int. Ed. Engl.*, 1981, **20**, 934.
17 S. D. Cumming, L. T. Cheng and R. Eisenberg., *Chem. Mater*, 1997, **9**, 440.
18 J. C. Calabrese, L. T. Cheng, J. C. Green, S. R. Marder and W. Tam, *J. Am. Chem. Soc.*, 1991, **113**, 7227.
19 R. Herrmann, B. Pedersen, G. Wagner and J. H. Youn, *J. Organomet. Chem.*, 1998, **571**, 261.
20 F. A. Cotton and R. A. Walton, *Multiple Bonds Between Metal Atoms*, Wiley, New York, 1982.
21 M. Sheik-bahae, A. A. Said, T. H. Wei, D. J. Hangan and E. W. Van Stryland, *IEEE J. Quant. Electron.*, 1990, **26**, 760.
22 M. Sheik-bahae, A. A. Said and E. W. Van Stryland, *Opt. Lett.*, 1989, **14**, 955.
23 SAINT (Version 5.00), Bruker AXS Inc., Madison, WI, USA, 1998.
24 G. M. Sheldrick, SADABS, A program for Empirical Absorption Correction of Area Detector Data, University of Göttingen, Göttingen, Germany, 1996.
25 SHELXTL (Version 5.1, IRIX), Bruker Analytical X-ray Instruments, Madison, WI, USA, 1997.
26 TEXSAN, Version 1.10. MSC, Rigaku Molecular Structure Corporation, 9009 New Trails Drive, The Woodlands, TX 77381–5209, USA, 1999.
27 A. C. T. North, D. C. Philips and F. S. Mathews., *Acta Crystallogr., Sect. A*, 1968, **24**, 351.
28 G. M. Sheldrick, SHELXTL-PC (Version 5.10), Siemens Analytical Instruments, Inc., Madison, WI, 1997.
29 A. Muller, H. Bogge and U. Schimanski., *Inorg. Chim. Acta*, 1980, **45**, L249.
30 J.-G. Li, X.-Q. Xin, Z.-Y. Zhou and K.-B. Yu., *J. Chem. Soc., Chem. Commun.*, 1991, 250.
31 T. E. Muller, J. C. Green, D. M. P. Mingos, C. M. Mcpartlin, C. Whittingham, D. J. Williams and T. M. Woodroffe., *J. Organomet. Chem.*, 1998, **551**, 313.
32 R. F. Ziolo, A. P. Gaughan, Z. Dori, C. G. Pierpont and R. Eisenberg., *Inorg. Chem.*, 1971, **10**, 1289.
33 R. F. Ziolo, A. P. Gaughan, Z. Dori, C. G. Pierpont and R. Eisenberg., *J. Am. Chem. Soc.*, 1970, **92**, 738.
34 (*a*) M. Sherk-Bahae, A. A. Said, T. H. Wei, D. J. Hagan and E. W. Van Stryland, *IEEE J. Quantum Electron.*, 1990, **26**, 760; (*b*) M. Sherk-Bahae, A. A. Said and E. W. Van Stryland, *Opt. Lett.*, 1989, **14**, 955.
35 H.-G. Zheng, W. Ji, M. L. K. Low, G. Sakane, T. Shibahara and X.-Q. Xin., *J. Chem. Soc. Dalton Trans.*, 1997, **13**, 2357.
36 H.-W. Hou, D.-L. Long, X.-Q. Xin, X.-Y. Huang, B.-S. Kang, P. Ge, W. Ji and S. Shi., *Inorg. Chem.*, 1996, **35**, 5363.
37 H.-W. Hou, Y.-T. Fan, C.-X. Du, Y. Zhu, W.-L. Wang, X.-Q. Xin, M. K. W. Low, W. Ji and H. G. Ang, *Chem. Commun.*, 1999, 647 and references therein.
38 C. Zhang, Y.-L. Song, G.-C. Jin, G.-Y. Fang, Y.-X. Wang, S. S. S. Raj, H. K. Fun and X.-Q. Xin., *J. Chem. Soc., Dalton Trans.*, 2000, 1317.
39 C. Zhang, Y. Song, B. M. Fung, Z. Xue and X. Xin, *Chem. Commun*, 2001, 843.